Biochemistry

 Volume 40, Number 3 January 23, 2001

Accelerated Publications

Synthetic Inhibitors of the Processing of Pretransfer RNA by the Ribonuclease P Ribozyme: Enzyme Inhibitors Which Act by Binding to Substrate†

Yoshiaki Hori,‡ Elena V. Bichenkova,§ Amanda N. Wilton,§ Mohamed N. El-Attug,§ Seyed Sadat-Ebrahimi,§ Terumichi Tanaka,‡ Yo Kikuchi,‡ Michihiro Araki,|| Yukio Sugiura,|| and Kenneth T. Douglas*,§

School of Pharmacy and Pharmaceutical Sciences, University of Manchester, Manchester M13 9PL, U.K., Division of Bioscience and Biotechnology, Department of Ecological Engineering, Toyohashi University of Technology, Tempaku-cho, Toyohashi 441-8580, Japan, and Institute for Chemical Research, Kyoto University, Uji, Kyoto 611-0011, Japan

Received October 12, 2000; Revised Manuscript Received December 4, 2000

ABSTRACT: 2,2′-*p*-Phenylene bis[6-(4-methyl-1-piperazinyl)]benzimidazole, 2,2′-bis(3,5-dihydroxyphenyl)-6,6′-bis benzimidazole, and 2,2′-bis(4-hydroxyphenyl)-6,6′-bis benzimidazole are shown by UV−visible and fluorescence spectrophotometry to be strong ligands for tRNA, giving simple, hyperbolic binding isotherms with apparent dissociation constants in the micromolar range. Hydroxyl radical footprinting indicates that they may bind in the D and T loops. On the basis of this tRNA recognition as a rationale, they were tested as inhibitors of the processing of precursor tRNAs by the RNA subunit of *Escherichia coli* RNase P (M1 RNA). Preliminary studies show that inhibition of the processing of *Drosophila* tRNA precursor molecules by phosphodiester bond cleavage, releasing the extraneous 5′-portion of RNA and the mature tRNA molecule, was dependent on both the structure of the inhibitor and the structure of the particular tRNA precursor substrate for $tRNA^{Ala}$, $tRNA^{Val}$, and $tRNA^{His}$. In more detailed followup using the $tRNA^{His}$ precursor as the substrate, experiments to determine the concentration dependence of the reaction showed that inhibition took time to reach its maximum extent. I_{50} values (concentrations for 50% inhibition) were between 5.3 and 20.8 μM, making these compounds among the strongest known inhibitors of this ribozyme, and the first inhibitors of it not based on natural products. These compounds effect their inhibition by binding to the substrate of the enzyme reaction, making them examples of an unusual class of enzyme inhibitors. They provide novel, small-molecule, inhibitor frameworks for this endoribonuclease ribozyme.

In all organisms studied to date, the transfer RNA genes express tRNA as precursors requiring processing to give the functional tRNA molecules. This maturation of the tRNA 5′-terminus is effected by ribonuclease P (RNase P),[1] an endoribonuclease, formed in eubacteria from an RNA subunit of approximately 400 nucleotides and a 14 kDa protein subunit. The catalytic activity is provided by the RNA, which under suitable conditions can even cleave its substrate correctly in the absence of protein. The protein subunit appears to aid product release and reduce the level of rebinding of the matured tRNA to the enzyme (*1*). Some aminoglycosides inhibit RNase P (*2*), and given that RNase P is essential and exhibits differences between species (*3*),

† We are grateful to the British Council for a Collaborative Research Project Grant (K.T.D.), the Libyan General Secretariat of Education and Vocational Formation (M.N.E.A.), and the "Research for the Future" programme of the Japan Society for the Promotion of Science (Grant JSPS-RFTF97I00301 to Y.K.).

* To whom correspondence should be addressed: School of Pharmacy and Pharmaceutical Sciences, University of Manchester, Manchester M13 9Pl, U.K. Telephone: 44 (0)161 275 2371. Fax: 44 (0)161 275 2481. E-mail: Ken.Douglas@man.ac.uk.

‡ Toyohashi University of Technology.

§ University of Manchester.

|| Kyoto University.

[1] Abbreviations: DMSO, dimethyl sulfoxide; MPE-Fe(II), methidium-propyl-EDTA-Fe(II); RNase P, ribonuclease P.

10.1021/bi002378f CCC: $20.00
Published on Web 12/28/2000

it has been suggested that these antibiotics might serve as lead structures for drug design (*2*).

The structure of the catalytic RNA of the eubacterial RNase P contains many of the three-dimensional structural motifs of a mature tRNA molecule, at least in an incipient form (*4*−*8*). Thus, we decided to use the tRNA tertiary structure as a scaffold from which to initiate lead drug/inhibitor design against this ribozyme. However, there are rather few reversible and specific ligands known for tRNA (*9*). Porphyrins bind (*10*) in the TΨC arm of brewer's yeast $tRNA^{Phe}$ near residues T54 and Ψ55 (*11*). X-ray diffraction data for distamycin bound to tRNA show specific hydrogen bonds to G51, U52, and G53 with electrostatic links to phosphates P61−P63 in the same groove region in the T-stem (*12*). Our NMR data confirm that distamycin selectively line broadens imino proton resonances of G18 and ψ55 in this region (*13*). Such binding was also detected by theoretical calculations (*14*).

We have discovered recently that certain benzimidazole ligands bind reversibly to *Escherichia coli* $tRNA^{Phe}$ with micromolar apparent dissociation constants (*15*), preliminary studies implicating the T-stem groove of *E. coli* $tRNA^{Phe}$ in this region as a possible ligand-binding site for **2** (*13*). This T-loop region is also implicated in recognition by RNase P; e.g., disruption of the G53·C61 base pair significantly decreases the cleavage rate (*16*). The 2′-OH groups of riboses 54 and 55, important for catalysis, may interact specifically with groups in the RNase P RNA (*17*).

Thus, we tested tRNA ligands (**1b**−**d** and **2**−**4**) as inhibitors of the ribozyme of *E. coli* RNase P (M1 RNA) using a variety of tRNA precursor substrates in a preliminary evaluation. We now report that **2**−**4** offer lead inhibition of the activity of M1 RNA, although the inhibitions are caused by the unusual mechanism of the binding of **2**−**4** to the substrates. To our knowledge, these are the first synthetic organic ligands reported to inhibit the M1 RNA reaction, whose structures are not based on natural products.

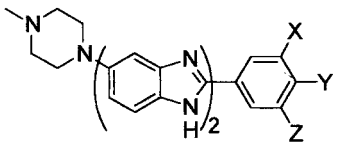

1a X=Z=H; Y=OH; Hoechst 33258
1b X=Y=H; Z=OH; SE 02
1c X=H; Y=OH; Z=OMe; SE11
1d X=Z=OH; Y=H; SE13

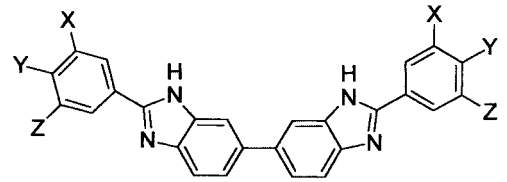

2 (X = Z = H : Y = OH)
3 (X = Z = OH: Y = H)

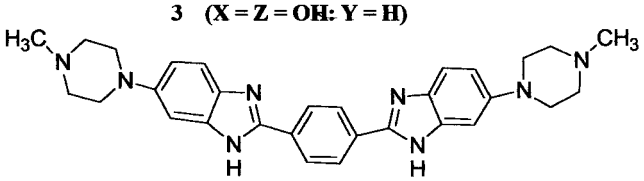

4

MATERIALS AND METHODS

*Synthesis of **2** and **3***. To a solution of 3,3′-diaminobenzidine (2.164 g, 10 mmol) in glacial acetic acid (40 mL) was added ethyl 4-hydroxybenzimidate hydrochloride (4.201 g, 20 mmol, 96% pure, Aldrich Chemical Co.), and the mixture was stirred over a water bath under reflux and nitrogen for 4 h to give a light-brown mixture. Acetic acid was removed by rotovap, the residue dissolved in hot water (10 mL), a mixture of 2-propanol and ammonia (10:1, 2 mL) added, and the resulting mixture stirred over a water bath for 1 h. The isolated precipitate was recrystallized from methanol to give a cream product (two crops, 3.52 g, 84%): mp >350 °C; ^{1}H NMR (270 MHz, DMSO-d_6] δ_H 6.95 (d, 4H, Ar-H, J = 8.6 Hz), 7.54 (d, 2H, Ar-H, J = 8.6 Hz), 7.66 (d, 2H, Ar-H, J = 8.6 Hz), 7.82 (s, 2H, Ar-H), 8.08 (d, 4H, Ar-H, J = 8.6 Hz), 10.5 (s, 2H, Ar-OH); electrospray MS (*m*/*z*, relative intensity) 420 (M + H + 1, 30%), 419 (M + H, 100%); TLC R_f 0.79 (30% NaOH/70% ethyl acetate), 0.75 (1:3 CH_2Cl_2/CH_3CN), 0.60 (3:1 CH_2Cl_2/MeOH). Anal. Calcd for $C_{26}H_{18}N_4O_2 \cdot H_2O$, CH_3OH, 2HCl: C, 59.9; H, 4.6; N, 10.1; Cl, 13.1. Found: C, 59.7; H, 4.7; N, 9.8; Cl, 12.8.

Similarly, **3** was prepared from 3,3′-diaminobenzidine (0.65 g, 3 mmol) and ethyl-3,5-dihydroxybenzimidate hydrochloride (1.30 g, 6 mmol) as a brown product (1.45 g, 89.3%): mp ≥350 °C; ^{1}H NMR (270 MHz, DMSO-d_6) δ_H 6.5 (s, 2H, Ar-H), 7.10 (d, 4H, Ar-H, J = 7.75 Hz), 7.75 (dd, 4H, Ar-H), 7.9 (s, 2H, Ar-H), 9.9 (s, 4H, Ar-OH); electrospray MS (*m*/*z*, relative intensity) 453 (M + H + 2, 5%), 452 (M + H + 1, 35%), 451 (M + H, 100%); TLC R_f 0.65 (3:1 CH_2Cl_2/MeOH), 0.41 (1:2 CH_2Cl_2/CH_3CN). Anal. Calcd for $C_{26}H_{18}N_4O_4$, CH_3OH, 2HCl: C, 58.3; H, 4.3; N, 10.1; Cl, 12.8. Found: C, 58.5; H, 4.4; N, 10.4; Cl, 13.0.

*Synthesis of **4***. 1,4-Benzene-bis-ethylimidate hydrochloride (586 mg, 2 mmol) was added to 4-*N*-piperidino-2-aminoaniline (824 mg, 4 mmol) in glacial acetic acid (5 mL) and refluxed under nitrogen with a $CaCl_2$ drying tube. Acetic acid was removed by rotavap, the residue dissolved in hot water (10 mL), and the solution filtered hot. The filtrate was evaporated by rotavap, the residue dissolved in MeOH (10 mL), triturated with ether, and filtered, and the solid purified as described for 3,4-dihydroxy-Hoechst (*18*) to give a brown-gray solid (650 mg, 64% yield): λ_{max} = 374 nm in MeOH; ^{1}H NMR (270 MHz, DMSO-d_6) δ_H 2.25 (s, 6H, N-CH_3), 3.14 (m, 8H, N-CH_2), 3.54 (m, 8H, N-CH_2), 6.97 (s, 2H, Ar-H), 7.49 (d, 2H, Ar-H, J = 7.25 Hz), 8.26 (s, 4H, Ar-H), 12.73 (brs 2H, NH); FAB MS (*m*/*z*, relative intensity) 509 (M + H + 2, 6.83), 508 (M + H + 1, 33), 507 (M + H, 100); accurate mass calcd for $C_{30}H_{35}N_8$ 507.2985, measured 507.2971 (error of 2.7 ppm). 1,4-Benzene-bis-ethylimidate hydrochloride was synthesized (*18*) from 1,4-dicyanobenzene (2.563 g, 20 mmol) in super-dry ethanol (8 mL) and anhydrous tetrahydrofuran (72 mL) with HCl gas at <10 °C as a white solid (3.23 g, 43.7%): mp 320−322 °C; ^{1}H NMR (270 MHz, DMSO-d_6) δ_H 1.49 (t, 6H, CH_3, J = 6.9 Hz), 4.65 (q, 4H, CH_2, J = 6.9 Hz), 7.9−8.4 (m, 4H, Ar-H), 12.1 (brs, 2H, NH); FAB MS (*m*/*z*, relative intensity) 223 (M + 2H + 1, 2.6), 222 (M + 2H, 21); accurate mass calcd for $C_{12}H_{18}N_2O_2$ 222.1368, measured 222.1366 (error of ≈1 ppm).

M1 RNA and tRNA Precursors. RNAs used in the M1 RNA reactions were prepared by in vitro transcription from the appropriate synthetic DNA or plasmids with T7 RNA polymerase (Toyobo). The tRNA precursors used for the preliminary studies of Figure 3 were labeled at the 3′-ends with [5′-^{32}P]pCp (Amersham) and T4 RNA ligase (Takara Shuzo Co.) as described previously (*19*, *20*).

Preliminary Screening Prior to the Assay for the RNase P Reaction. The standard, high-salt reaction mixture (H) contained 50 mM Tris-HCl (pH 7.6), 100 mM NH_4Cl, 60 mM $MgCl_2$, 5% (w/v) polyethylene glycol, 2 μg of M1 RNA, 0.6% (v/v) dimethyl sulfoxide (DMSO), and 2−5 fmol of 3′-end-labeled tRNA precursor in a total volume of 10 μL. Another mixture with a lower salt content (L) was also prepared (0 mM NH_4Cl and 10 mM $MgCl_2$). For the inhibition assay, **1b**−**d**, **2**, or **3** was added to the reaction mixture from a stock solution in DMSO to give a final concentration of 30 μM. This mixture was incubated at 37 °C for 1 h and the reaction stopped by addition of 0.5 M EDTA (2 μL). The products were separated by electrophoresis (20% polyacrylamide−8 M urea gel) and detected by autoradiography (*19*), and products were assayed using a PhosphorImager (Molecular Dynamics). In the assay of RNase P, the DMSO level is kept low as it affects the kinetic parameters at high percentages [K_i for DMSO is 4 M (*21*)].

Concentration Dependence of the Inhibition of RNase P. The M1 RNA solution contained 50 mM Tris-HCl (pH 7.6), 100 mM NH_4Cl, 60 mM $MgCl_2$, 5% (w/v) polyethylene glycol 6000, 0.6% (v/v) DMSO, and 24.3 nM M1 RNA. The substrate ($tRNA^{His}$ precursor) solution contained 50 mM Tris-HCl (pH 7.6), 100 mM NH_4Cl, 60 mM $MgCl_2$, 5% (w/v) polyethylene glycol, 0.6% (v/v) DMSO, and 4.66 nM substrate. Both mixtures were separately preincubated at 37 °C for 90 min in the presence and absence of inhibitors (0.9375−30 μM). This preincubation is necessary to obtain reproducible M1 RNA kinetic data as well as maximal inhibition by these inhibitors. The reaction was initiated by adding substrate solution (10 μL) to M1 RNA solution (2.5 μL), giving a final volume of 12.5 μL and giving final concentrations of M1 RNA and substrate in the reaction mixture of 4.85 and 3.73 nM, respectively. The mixture was incubated at 37 °C for 5 min and the reaction stopped by addition of EDTA (4 μL of a 0.5 M solution). The products were fractionated on a 20% (w/v) denaturing polyacrylamide gel and visualized by using a PhosphorImager (Molecular Dynamics). Quantitative analyses of reaction products were performed by counting photostimulated luminescence of the product bands in radiograms of the gel with the PhosphorImager.

MPE-Fe(II) Footprinting. MPE-Fe(II) stock solutions were prepared freshly prior to use by mixing 2 nmol of MPE (Sigma) and 500 pmol of ferrous ammonium sulfate. *E. coli* (Sigma Chemical Co.) $tRNA^{Val}$ (5′-end-labeled, 15 000 cpm) prepared as described previously (*22*, *23*) was denatured at 70 °C for 1 min in reaction buffer containing 2 μg of carrier tRNA, 10 mM cacodylic acid, 1 M NaCl, and 50 mM $MgCl_2$ at pH 7.0. After renaturation by cooling to room temperature, various concentrations of ligands and the MPE-Fe(II) solution were added to a final volume of 20 μL and the reaction mixtures incubated at 30 °C for 10 min. The oxidative cleavage reactions were initiated by adding dithiothreitol (final concentration of 10 mM) and incubating at 30 °C for 30 min. The reactions were terminated by adding carrier tRNA (2 μg), followed by ethanol precipitation. The precipitated samples were analyzed on 15% polyacrylamide−7 M urea gels. The full-length $tRNA^{Val}$ and G-specific cleavage products (from RNase T1) were co-electrophoresed. Results were visualized by autoradiography.

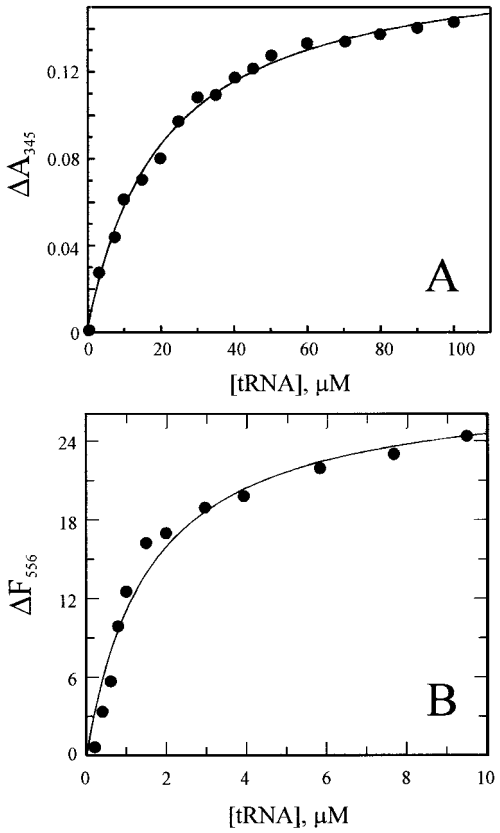

FIGURE 1: (A) Titration curve showing the change in the absorbance at 345 nm (ΔA_{345}) vs the concentration of $tRNA^{Phe}$ for **2** (20 μM) in 0.1 M HEPES and 1 M NaCl (pH 7.00). Points are experimental; the line is theoretical with a K_{diss} of 16.1 ± 1.4 μM and a maximal absorbance change of 0.253 and the equation $A = A_{max}[tRNA^{Phe}]/(K_{diss} + [tRNA^{Phe}])$. (B) Fluorescence titration curve for **4** (10 μM) in 0.01 M cacodylate, 1 M NaCl, and 0.05 M $MgCl_2$ (pH 7.0) showing the change in fluorescence intensity at 556 nm (ΔF_{556}) vs the concentration of $tRNA^{Phe}$. Points are experimental; the line is theoretical assuming hyperbolic binding with a K_{diss} of 1.6 ± 0.3 μM and a maximal relative fluorescence change of 28.4.

RESULTS

UV−Visible Spectrophotometric Studies of Binding to tRNA. The ligands that were studied were shown to bind strongly to $tRNA^{Phe}$ by monitoring their UV−visible absorption spectra in their region of maximum absorbance (λ_{max}). A shift from 325 to 342 nm was observed for **2** in 0.1 M Tris, 0.1 M NaCl, and 0.01 M $MgCl_2$ (pH 7.5) and from 330 to 355 nm in 0.1 M HEPES and 0.1 M NaCl (pH 7.00). For **4**, a shift from 359 to 375 nm was observed in 0.1 M Tris, 0.1 M NaCl, and 0.01 M $MgCl_2$ (pH 7.5). UV−visible absorption spectral titration was carried out for **2** (20 μM) in 0.1 M HEPES and 0.1 M NaCl (pH 7.00) between 280 and 430 nm by addition of aliquots of $tRNA^{Phe}$, to a final $tRNA^{Phe}$ concentration of 100 μM. After correction for dilution, the change in absorbance at 345 nm (ΔA) plotted versus the concentration of $tRNA^{Phe}$ (Figure 1A) gave a

dissociation constant (K_{diss}) for **2** with tRNA^{Phe} of 16.1 ± 1.4 μM, assuming a single binding site, or noncooperative binding at more than 1 site, and a hyperbolic binding equation. For 20 μM **4** in 0.1 M Tris, 0.1 M NaCl, and 0.01 M $MgCl_2$ (pH 7.5), UV−visible titration gave a K_{diss} value of 3.04 ± 0.35 μM.

Spectrofluorimetric Evidence of Binding to tRNA. On interaction of tRNA and the ligand, changes are seen in the fluorescence emission spectra of ligands **2**−**4**. For **2** in cacodylate buffer, a shift in the emission maximum from 388 to 395 nm was observed; for **4**, the shift was from 555 to 550 nm. In this particular buffer, this addition is also associated with quenching of the fluorescence of the free ligand.

The fluorescence of tRNA^{Phe} is weak, but there is potential interference from the Y base in its T-loop. It was possible to minimize this by exciting the ligand at a wavelength that left the fluorescence of the free tRNA^{Phe} relatively unchanged. Thus, the observed fluorescence intensity (F) could be attributed to the relative concentrations of the free and bound ligand and any changes to formation of a complex(es), described by $F = F_{max}[tRNA^{Phe}]/(K_{diss} + [tRNA^{Phe}])$, here written for noninteracting binding sites. Spectrofluorimetric titration was carried out in 0.01 M cacodylic acid and 0.05 M $MgCl_2$ (pH 7.0) with 1 M NaCl to minimize the possibility of nonspecific electrostatic interactions. In this buffer, the emission λ_{max} of **4** alone (555 nm) shifted to 550 nm for the equimolar ligand and tRNA^{Phe}, with progressive quenching for successive additions of tRNA^{Phe}. From the plot of the change in fluorescence (ΔF) versus the amount of tRNA^{Phe} added (Figure 1B), the apparent K_{diss} value for the complex of **4** with tRNA^{Phe} was 1.6 ± 0.3 μM using the simple binding equation. For **2** in 0.1 M sodium phosphate (pH 7.8), the fluorescence signal was enhanced on adding tRNA^{Phe} and the hyperbolic plot of ΔF versus the amount of tRNA^{Phe} added gave an apparent K_{diss} for the complex of **2** with tRNA^{Phe} of 0.692 ± 0.156 μM, using the simple binding equation. The same experiment carried out in 0.01 M cacodylic acid, 1 M NaCl, and 0.05 M $MgCl_2$ (pH 7.0) produced a decrease in fluorescence intensity on addition of tRNA^{Phe} (apparent K_{diss} = 3.9 ± 0.6 μM).

Footprinting Studies. Identification of binding regions for the ligands on the tRNA by direct NMR studies, as carried out for the imino and other protons of tRNA with distamycin (*13*), was precluded because of precipitation. Therefore, hydroxyl radical-derived footprinting studies were carried out, based on the potential of these ligands to protect against cleavage of tRNA by the MPE-Fe(II) system, in an attempt to detect the binding site(s) of these ligands on tRNA. This small molecule provides a useful structure-based chemical probe and has shown greater access to tRNA structure than bulky enzymatic probes (*24*, *25*). Figure 2 shows the result for 5′-end-labeled tRNA^{Val} in the presence of the MPE-Fe(II) solution and various concentrations of **2**−**4**. Virtually every position in the tRNA^{Val} molecule appeared to be sensitive to MPE-Fe(II)-catalyzed cleavage (lane 3). Titration with increasing amounts of the ligands showed that some specific cleavages seen in lane 3 lost prominence in the presence of excess ligands (lanes 4−12). The concentrations of the ligands were 1−100 times greater than the K_{diss} values measured in the spectroscopic studies, and hence, solubility problems arose, especially for **3**. Although the protection is

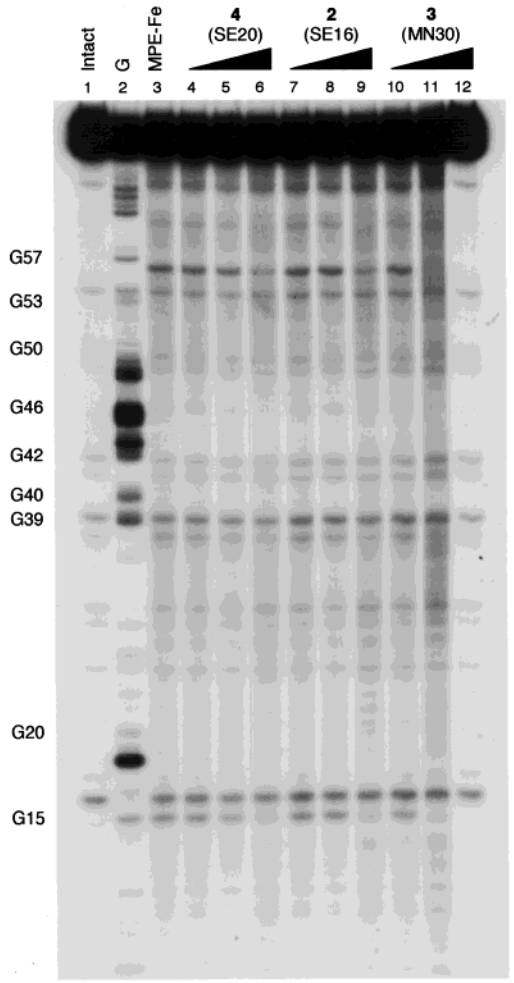

FIGURE 2: MPE-Fe(II) footprint titration of **2**−**4** with 5′-^{32}P-end-labeled *E. coli* tRNA^{Val}: lane 1, intact tRNA^{Val}; lane 2, RNase T1 G-track; lane 3, MPE-Fe(II) standard; lanes 4−6, 1, 10, and 100 μM **4** (SE20), respectively; lanes 7−9, 1, 10, and 100 μM **2** (SE16), respectively; lanes 10−12, 1, 10, and 100 μM **3** (MN30), respectively.

weak, the protection effects depended on the particular tRNA that was studied, but for tRNA^{Val} (Figure 2), protection was seen for **2**−**4** around residue G15 located in the D-loop and residue C56 in the T-loop. There also appears to be weak protection at nucleotides 60 and 46 near the T-loop. Under these experimental conditions, tRNA exists in a highly structured state with tertiary interactions between nucleotides in the D-loop and the T-loop. Binding of ligands **2**−**4** to a specific site in tRNA perturbed the interaction of both loops so that inhibition of the MPE-Fe(II) reaction could be observed in the loop regions.

Inhibition of the M1 RNA Reaction. Preliminary results on the effects of some of the ligands on M1 RNA activity are summarized in Figure 3, an autoradiogram of the gel for pre-tRNA^{His}. The strongly detected band at the top of the gel corresponds to substrate pre-tRNA^{His}, and sites of cleavage are indicated by partial alkaline hydrolysis (lanes 1 and 16) and ribonuclease T1 partial digestion (lane 17). Cleavage to mature tRNA^{His} is favored by high-salt conditions [compare bands 3(L) and 4(H)] and requires the presence of M1 RNA (lane 2 vs lane 3). There is no detectable inhibition of conversion of pre-tRNA^{His} to mature tRNA^{His} for **1b** (lane 7 vs lane 5), **1c**, or **1d**. However, **2** and **4** (lanes 13 and 15, respectively) both show that much

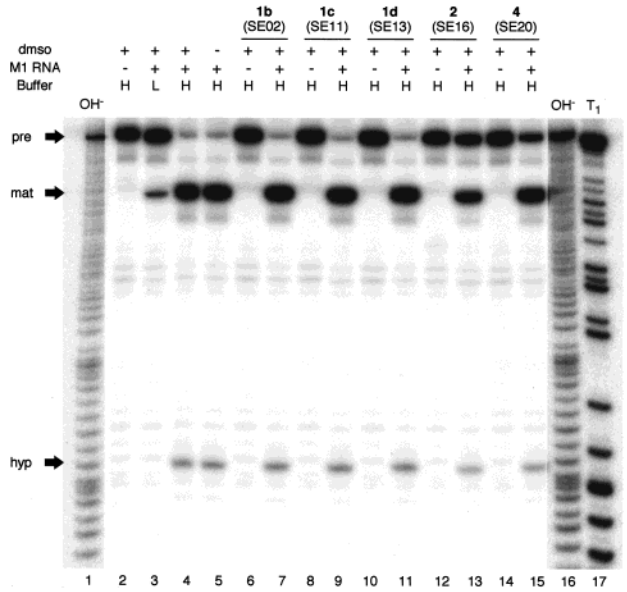

FIGURE 3: Denaturing gel electrophoresis (20% PAGE−8 M urea gel) for the processing of *Drosophila* pre-tRNA^{His} ($\sim 10^{-7}$ M) by M1 RNA (0.78 μM, *E. coli* RNase P RNA component) by **1b** (SE02), **1c** (SE11), **1d** (SE13), **2** (SE16), and **4** (SE20) at 30 μM in the presence of 0.6% (v/v) DMSO in H (high-salt) buffer consisting of 60 mM $MgCl_2$, 100 mM NH_4Cl in 50 mM Tris-HCl (pH 7.6), and 5% (w/v) polyethylene glycol. Lane 3 contained in low-salt (L) buffer consisting of 50 mM Tris-HCl (pH 7.6) and 5% polyethylene glycol, with 10 mM $MgCl_2$ and no NH_4Cl present. The pre and mat bands indicate precursor and mature tRNA, respectively. The hyp band indicates the internally cleaved by-product (hyperprocessed product) [see Hori et al. (*31*)]. The labels T_1 (lane 17) and OH^- (lanes 1 and 16) represent partially cleaved products from the action of RNase T1 and alkaline hydrolysis, respectively. The autoradiograms that are shown are from a PhosphorImager (Molecular Dynamics). The band nearest the top of the gel is the pre-tRNA^{His} [indicated by the heavy band and top arrow near the OH^- alkaline partial digest lane on the left of the gel (lane 1)]; the next heavy band (see lane 2 or 3) is the mature tRNA body.

less pre-tRNA^{His} has been processed. As in the case of pre-tRNA^{His}, **1b** did not show any inhibition of the processing reactions of tRNA^{Ala} or pre-tRNA^{Val}, while both **2** and **4** acted to different extents as inhibitors for the processing reactions of these two pre-tRNAs (data not shown). Under these initial conditions, the sensitivity of M1 RNA cleavage to the particular tRNA varied with both the pre-tRNA that was used and inhibitor structure.

More detailed followup showed that inhibition was time-dependent, optimal inhibition requiring preincubation of the inhibitors with the substrate, with preincubation for 10−60 min with precursor tRNA substrates being necessary to obtain maximal inhibition. (Preincubation of the compounds with M1 RNA had almost no effect on the cleavage reaction.) Preincubation of our M1 RNA preparation with Mg^{2+} and NH_4^+ is also necessary to obtain reproducible kinetic data. Consequently, the concentration dependencies of inhibition were studied with a 90 min preincubation of the inhibitor with all components of the assay (see Materials and Methods). Compounds **1b**−**d** exhibited no inhibition up to 30 μM each. However, **2**−**4** exhibited strong inhibition with I_{50} values (concentration giving 50% inhibition under the assay conditions described here) of 8.55, 5.33, and 20.8 μM, respectively (see Figure 4A−C). A repeat for **2** (from a separate synthesis) gave a value of 7.89 μM, indicating good reproducibility.

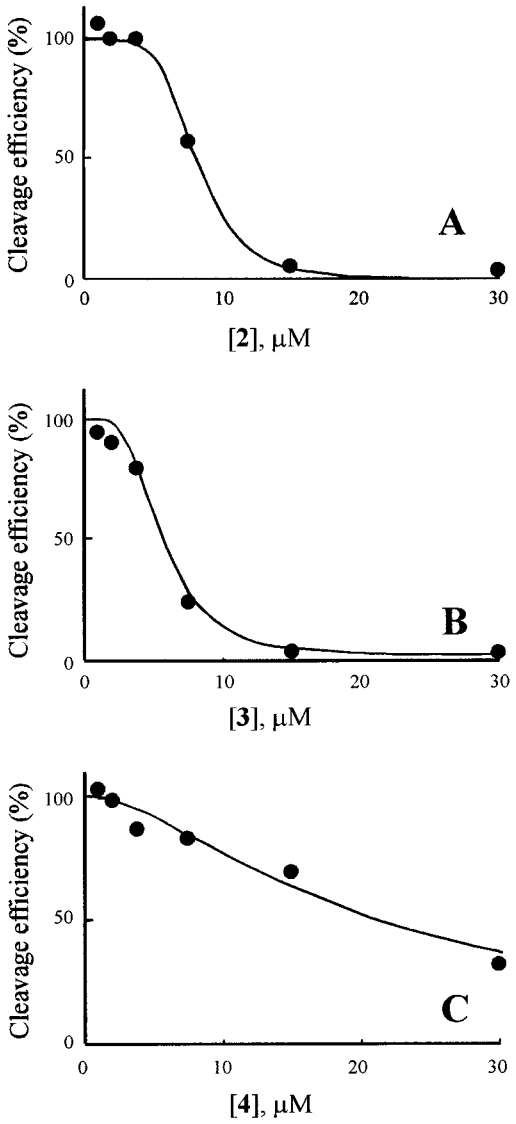

FIGURE 4: Inhibition of 3.73 nM *Drosophila melanogaster* pre-tRNA^{His} and the M1 RNA component of *E. coli* RNase P by (A) **2**, (B) **3**, and (C) **4**, as described in Materials and Methods.

DISCUSSION

Evidence for the binding of the ligands in this study to tRNA comes from absorbance spectrophotometry, spectrofluorimetry, and footprinting measurements, in addition to literature data for some of the compounds (*13*, *15*). The shift in the absorbance maximum to a longer wavelength for **2**−**4** indicates a change in the microenvironment of the ligand and tRNA. Binding is also demonstrated by the concentration dependencies of the change in absorption intensity. In addition, the interaction of ligands with tRNA is accompanied by shifts in the maximal wavelength of fluorescence emission, observed for **2** and **4**. The K_{diss} values obtained for the binding of tRNAs to **2**−**4** are approximately micromolar. For **2** with tRNA, K_{diss} is 0.6 μM (*13*), and for the dimethoxy variant of **1** (X and Y, MeO; Z, H), K_{diss} is 14.8 μM (*15*). The footprinting data are consistent with the main binding sites for **2**−**4** being in the D- and T-loops. In *Bacillus subtilis* RNase P, there is evidence that the T-stem−loop portion of a pre-tRNA substrate is highly structured when it interacts with the P RNA (*16*). The D-arm also contributes to the recognition by RNase P (*26*). While it is not possible to

obtain K_i values from I_{50} data without knowing the type of inhibition or substrate concentrations and K_m values, the levels of M1 RNA inhibition achieved here are consistent with these classes of ligands binding to the groove(s) of tRNA structures recognized for productive substrate action by M1 RNA.

The inhibition by **2**−**4** is dependent on the particular pre-tRNA used, consistent with a specific mode of inhibition. The inhibition is very sensitive to the detailed chemical structures of the tRNA-derived ligand [the Hoechst 33258 analogues **1a**−**d** are ineffective inhibitors of M1 RNA in the present system despite members of their structural family binding to yeast tRNA (*15*)]. The differences in the strength of inhibition between **2** or **3** and **4**, again from differing structural families, indicate that specific structural attributes are required for strong inhibition of M1 RNA. Inhibition by these synthetic ligands is certainly stronger than, or comparable with, inhibition (*2*) for the aminoglycosides (I_{50} values against RNase P from 35 to 275 μM). Retinoids are competitive inhibitors of RNase P from *Dictostelium discoideum* with K_i values ranging from 8 to 1475 μM [and IC_{50} values under the conditions that were used (*21*) of 40−500 μM]. It was proposed that these hydrophobic retinoids, bearing no structural similarity to tRNA, may bind to allosteric inhibition sites of the enzyme, but these have not yet been defined in terms of their location.

Cleavage of pre-tRNA is inhibited by various aminoglycosides, most strongly by neomycin B (*2*). Studies in tandem with Pb(II) cleavage experiments indicated that the neomycin B interferes with divalent metal ion binding to the RNA, suggesting competition for the functionally relevant Mg^{2+} binding sites. Although it is not yet clear exactly how **2**−**4** inhibit M1 RNA action, they appear to inhibit by binding directly to the tRNA precursor substrate molecules. This makes them an uncommon class of enzyme inhibitors. Inhibition is unlikely to be the result of a metal ion displacement, as proposed for the natural antibiotics neomycin B, paromomycin, and the kanamycins (*2*), as there is no obvious common metal ion chelation mechanism for **2**, **3**, or **4**. Another possibility is that critical Mg^{2+} ions may be excluded from the productive ribozyme conformation, but this would have to be a result of a primary binding of ligands **2**−**4** to the (incipient) tRNA-like groove sites. There are Mg^{2+} ion binding sites in the D-loop−T-loop domain of yeast $tRNA^{Phe}$ (*27*), and such sites have been putatively advanced as a potential contributor to inhibition by neomycin B in RNase P (*2*, *28*). However, in preliminary studies, we have found that compounds **2**−**4** and Mg^{2+} do not compete in the M1 RNA reaction.

For these slow-acting inhibitors, it is important to determine the molecular basis of the slow onset. The fact that the inhibition is maximal after prolonged incubation suggests some type of conformational change induced in one or more components of the systems by these new inhibitors. The ligands discovered here may be serving as templates to induce a particular conformation which leads to inhibition. This is likely to be a different type of process to the change in conformation suspected for the tRNA component when *Drosophila* initiator methionine tRNA is hyperprocessed by M1 RNA (*17*, *20*, *29*−*31*).

Our findings extend the chemical structures available for the design of ligands of RNase P which may serve as potential drug leads, and introduce frameworks considerably less complex, and hence synthetically more accessible, than aminoglycosides. They may also provide probes of the system as they are amenable to chemical alteration.

REFERENCES

1. Kirsebom, L. (1998) in *The Many Faces of RNA* (Eggleston, D. S., Prescott, C. D., and Pearson, N. D., Eds.) pp 127−144, Academic Press, New York.
2. Mikkelsen, N. E., Brannvall, M., Virtanen, A., and Kirsebom, L. (1999) *Proc. Natl. Acad. Sci. U.S.A. 96*, 6155−6160.
3. Frank, D. N., and Pace, N. R. (1998) *Annu. Rev. Biochem. 67*, 153−180.
4. Massire, C., Jaeger, L., and Westhof, E. (1998) *J. Mol. Biol. 279*, 773−793.
5. Westhof, E., Wesolowski, D., and Altman, S. (1996) *J. Mol. Biol. 258*, 600−613.
6. Westhof, E., and Altman, S. (1994) *Proc. Natl. Acad. Sci. U.S.A. 91*, 5133−5137.
7. Harris, M. E., Nolan, J. M., Malhotra, A., Brown, J. W., Harvey, S. C., and Pace, N. R. (1994) *EMBO J. 13*, 3953−3963.
8. Harris, M. E., Kazantsev, A. V., Chen, J.-L., and Pace, N. R. (1997) *RNA 3*, 561−576.
9. Douglas, K. T. (1998) in *Structure, Motion, Interaction and Expression of Biological Macromolecules, Proceedings of the 10th Conversation, SUNY, Albany, NY, 1997* (Sarma, R. H., and Sarma, M. H., Eds.) pp 279−293, Adenine Press, Schenectady, NY.
10. Foster, N., Singhal, A. K., Smith, M. W., Narcos, N. G., and Schray, K. J. (1988) *Biochim. Biophys. Acta 950*, 118−131.
11. Birdsall, W. J., Anderson, W. R., Jr., and Foster, N. (1989) *Biochim. Biophys. Acta 1007*, 176−183.
12. Rubin, J., and Sundaralingam, M. (1984) *J. Biomol. Struct. Dyn. 2*, 165−174.
13. Bichenkova, E. V., Sadat-Ebrahimi, S. E., Wilton, A. N., O'Toole, N., Marks, D. S., and Douglas, K. T. (1998) *Nucleosides Nucleotides 17*, 1651−1665.
14. Zakrzewska, K., and Pullman, B. (1984) *J. Biomol. Struct. Dyn. 2*, 737.
15. Sadat-Ebrahimi, S. E., Wilton, A. N., and Douglas, K. T. (1997) *J. Chem. Soc., Chem. Commun.*, 385−386.
16. Loria, A., and Pan, T. (1997) *Biochemistry 36*, 6317−6325.
17. Krupp, G. (1993) *Biochimie 75*, 135−139.
18. Parkinson, J. P., Sadat-Ebrahimi, S., Wilton, A., McKie, J. H., Andrews, J., and Douglas, K. T. (1995) *Biochemistry 34*, 16240−16244.
19. Kikuchi, Y., and Sasaki, N. (1992) *J. Biol. Chem. 267*, 11972−11976.
20. Kikuchi, Y., Sasaki, N., and Ando-Yamagami, Y. (1990) *Proc. Natl. Acad. Sci. U.S.A. 87*, 8105−8109.
21. Papadimou, E., Georgiou, S., Tsambaos, D., and Drainas, D. (1998) *J. Biol. Chem. 273*, 24375−24378.
22. Araki, M., Okuno, Y., Hara, Y., and Sugiura, Y. (1998) *Nucleic Acids Res. 26*, 3379−3384.
23. Sugiura, Y., Totsuka, R., Araki, M., and Okuno, Y. (1997) *Bioorg. Med. Chem. 5*, 1229−1234.
24. Vary, C. P. H., and Vournakis, J. N. (1984) *Proc. Natl. Acad. Sci. U.S.A. 81*, 6978−6982.
25. Hertzberg, R. P., and Dervan, P. B. (1982) *J. Am. Chem. Soc. 104*, 313−315.
26. Hardt, W.-D., Schlegl, J., Erdmann, V. A., and Hartmann, R. K. (1993) *Biochemistry 32*, 13046−13053.
27. Holbrook, S. R., Sussman, J. L., Warrant, R. W., Church, G. M., and Kim, S.-H. (1977) *Nucleic Acids Res. 4*, 2811−2820.
28. Hermann, T., and Westhof, E. (1998) *J. Mol. Biol. 276*, 903−912.
29. Kikuchi, Y. (1996) *Mol. Biol. Rep. 22*, 171−175.
30. Hori, Y., Tanaka, T., and Kikuchi, Y. (2000) *FEBS Lett. 472*, 187−190.
31. Hori, Y., Baba, H., Ueda, R., Tanaka, T., and Kikuchi, Y. (2000) *Eur. J. Biochem. 267*, 4781−4788.

BI002378F